

Efficient visible photoinitiator with high-spectrum stability in an acid medium for free-radical and free-radical-promoted cationic photopolymerization based on erythrosine B derivatives

Xuying Nan,^{1,2} Yi Huang,² Qinguo Fan,³ Jianzhong Shao,² Yuhua Yao¹

¹College of Life Sciences, Zhejiang Sci-Tech University, Hangzhou 310018, China

²Engineering Research Center for Eco-Dyeing and Finishing of Textiles (Ministry of Education), Zhejiang Sci-Tech University, Hangzhou 310018, China

³Department of Bioengineering, University of Massachusetts Dartmouth, North Dartmouth, Massachusetts 02747

Correspondence to: J. Shao (E-mail: jshao@zstu.edu.cn)

ABSTRACT: Three dye-linked photoinitiators with excellent spectral stability in an acid medium were synthesized by the covalent bonding of a coinitiator (tertiary amine) and a benzoyl group or two coinitiators to the phenolic and carboxyl group position of erythrosine B. The combination of the iodonium salt and free tertiary amino used to initiate the free-radical/cationic visible photopolymerization was investigated to acquire the relationship between the structure and performance. The photoinitiating ability of the derivative with the phenolic position bearing a coinitiator was poorer than of the derivative with the carboxyl group bearing one because of the strong back electron transfer of the former. For the derivative with a linked coinitiator on the carboxyl position, the proximity effect between the sensitizer and the coinitiator moiety resulted in an excellent photoinitiating ability for radical/cationic polymerization; this suggested its potential for application. Although radical/cationic photopolymerization could be initiated by the derivative/coinitiator/iodonium salt, the different component ratios between them had different effects on these two polymerizations; this provided useful information for the design of effective photoinitiators for different polymerizations. On the basis of the fluorescence quenching and photopolymerization results, a corresponding synergistic mechanism was proposed. © 2015 Wiley Periodicals, Inc. *J. Appl. Polym. Sci.* **2016**, *133*, 43035.

KEYWORDS: differential scanning calorimetry (DSC); photochemistry; photopolymerization; radical polymerization; ring-opening polymerization

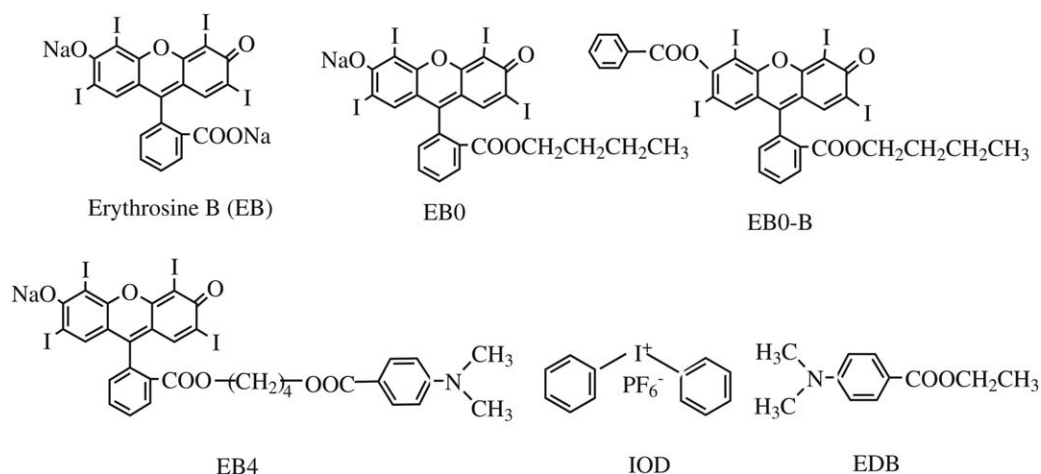
Received 9 July 2015; accepted 11 October 2015

DOI: 10.1002/app.43035

INTRODUCTION

UV-light-induced photopolymerization has been applied industrially in the fields of coatings, printed circuits, printing inks, and adhesives. However, some issues associated with UV curing, such as the generation of ozone, radiation safety, and curing depth, hinder its further application.¹ Because of this, visible-light-induced photopolymerization were proposed in the 1970s and has received extensive attention. At present, it is commercially applied only in dentistry. The search for new photoinitiators and/or photoinitiating systems for free-radical polymerization, cationic polymerization, and free-radical-promoted cationic polymerization is the subject of many published works.² The modification of the existing photoinitiator and the search for new dye skeletons as photosensitizers are two main strategies for the design of new visible photoinitiating systems.

Some dyes, such as acridine orange, eosin B, erythrosin B, rose bengal, rhodamine B, and methylene blue, used as visible photosensitizers have been extensively reported.³ As one of them, erythrosine B in combination with a hydrogen donor (typically a tertiary amine) is well known for initiating free-radical photopolymerization.⁴ To enhance the photoinitiating efficiency, an iodonium salt was incorporated into this two-component system; this system proved to be extremely sensitive and efficient for free-radical photopolymerization. A detailed study was done on the synergistic mechanism.^{5–7} In addition, this system, composed of erythrosine B, tertiary amine, and iodonium salt, could also initiate the cationic photopolymerization of epoxy monomer.⁸ However, how the photoinitiating efficiency of free-radical or cationic photopolymerization is affected by the proportions of these three components remains unclear. The mechanism for producing cationic active centers has also been described in various ways.



Scheme 1. Structures of some of the materials used in this study.

The photopolymerization formulation is usually a hydrophobic system, and erythrosine B as the water-soluble dye cannot fully dissolve in it; this prevents its application in these systems. In addition, erythrosine B is very sensitive to environmental pH, and its absorption spectrum changes dramatically, especially in an acid medium; this brings a great deal of difficulty to choosing a matching light source for photopolymerization.

In this study, through the modification of the two susceptible groups of erythrosine B with a coinitiator (4-dimethyl aminobenzoyl chloride) or benzoyl chloride, respectively, three hydrophobic derivatives with excellent spectrum stabilities in acid media were synthesized. These derivatives, combined with iodonium salt and free tertiary amino, were investigated to obtain the relationship of the structure and performance for initiating free-radical/cationic photopolymerization, and acquire the information on the effect of the component ratios on the two photopolymerizations. The photobleaching behaviors and the fluorescence quenching of different systems were investigated. On the basis of these results, a reasonable initiating mechanism was proposed.

EXPERIMENTAL

Materials

Erythrosine B disodium salt (EB), 4-(dimethyl amino) benzoyl chloride, and benzoyl chloride were purchased from Aladdin Chemistry Co., Ltd. Ethyl 4-dimethyl aminobenzoate (EDB) was purchased from TCI Shanghai. Anhydrous pyridine was purchased from Maya Reagent Co., Ltd. 1,6-Hexanediol diacrylate (HDDA; Aladdin) and 3,4-epoxycyclohexylmethyl 3',4'-epoxycyclohexane carboxylate (UVR; Shanghai Macklin Biochemical Co., Ltd.) were used as received. Diphenyliodonium hexafluorophosphate (IOD) was purchased from Sigma-Aldrich Chemistry. An erythrosine B derivative with a linked coinitiator on the carboxyl group (EB4), erythrosine B butyl ester (EBO), and erythrosine B derivative with shielded carboxyl and hydroxyl groups (EB0-B) were synthesized by our laboratory. Other chemicals were analytical grade except as noted. The structures of some of the materials used in this study are illustrated in Scheme 1.

Synthesis of the Erythrosine B Derivatives

EBO and EB4 reacted with 4-dimethyl aminobenzoyl chloride, respectively to obtain the derivatives, which was abbreviated as

EB0-EDB and EB4-EDB, respectively. EB4 reacted with benzoyl chloride to obtain the derivative, which was abbreviated as EB4-B. They were synthesized according to Scheme 2.

Synthesis of EB0-EDB and EB4-EDB. EB0 (1.09 mmol) and 4-(dimethyl amino) benzoyl chloride (1.63 mmol) were dissolved in 20 mL of dichloromethane in an ice bath, to which 1.5 mL of anhydrous pyridine was added dropwise. We stirred the reaction mixture at room temperature until the end of the reaction with thin chromatograph detection with dichloromethane as a developing agent. After the end of the reaction, the mixture was concentrated by a rotary evaporator and was then purified by flash chromatography (200–300 silica gel with dichloromethane as the eluent). The collected eluent was dried by rotary evaporation to obtain the erythrosine B derivative (EB0-EDB), and the synthesis data were as follows:

Yield = 85%. $^1\text{H-NMR}$ (CDCl_3 , 400 MHz, δ): 6.78–8.16 (10H, aromatic), 4.08–4.11 (2H, $-\text{COOCH}_2-$), 3.12 [6H, $-\text{N}(\text{CH}_3)_2$], 1.16–1.26 (4H, $-\text{CH}_2\text{CH}_2-$), 0.85–0.89 (3H, $-\text{CH}_3$). Electrospray ionization mass spectrometry (ESI-MS) $[\text{EB0-EDB} + \text{Na}^+]^+$: theoretical, 1062.05; detected, 1061.95.

EB4-EDB was synthesized via the same procedure, and the synthesis data were as follows.

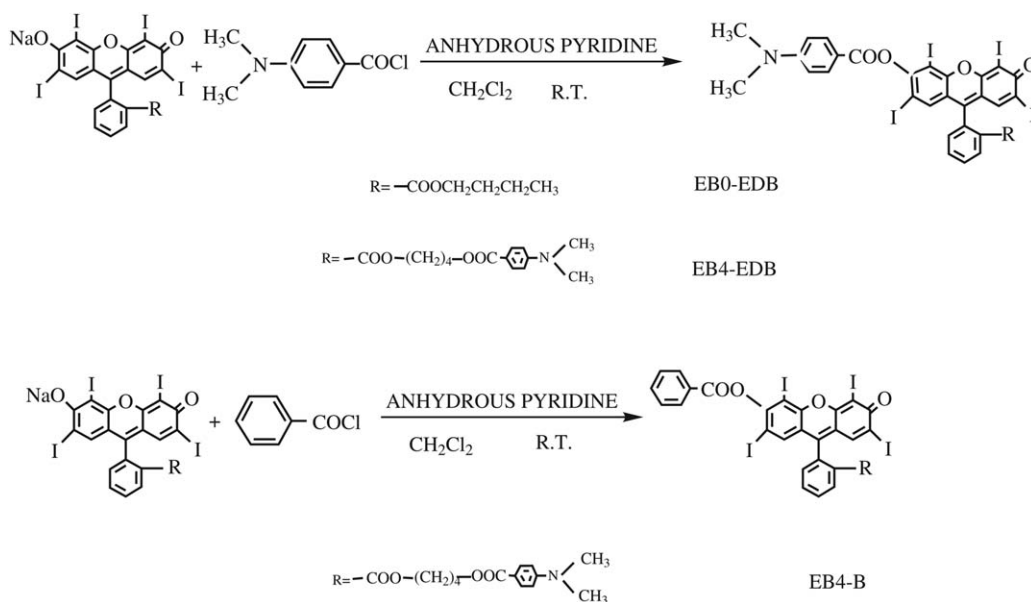
Yield = 52%. $^1\text{H-NMR}$ (CDCl_3 , 400 MHz, δ): 6.69–7.84 (14H, aromatic), 4.18–4.27 [4H, $(-\text{COOCH}_2-)_2$], 3.04–3.11 [12H, $[-\text{N}(\text{CH}_3)_2]_2$], 1.26 [4H, $(-\text{CH}_2-)_2$]. ESI-MS $[\text{EB4-EDB} + \text{Na}^+]^+$: theoretical, 1225.05; detected, 1225.19.

Synthesis of EB4-B. EB4-B was synthesized via the previous method, and the only difference was that the acylation reaction was performed between EB4 and benzoyl chloride. The synthesis data were as follows:

Yield = 65%. $^1\text{H-NMR}$ (CDCl_3 , 400 MHz, δ) = 6.69–7.84 (15H, aromatic), 4.19–4.28 [4H, $(-\text{COOCH}_2-)_2$], 3.04 [6H, $-\text{N}(\text{CH}_3)_2$], 1.24–1.28 [4H, $(-\text{CH}_2-)_2$]. ESI-MS $[\text{EB4-B} + \text{Na}^+]^+$: theoretical, 1181.86; detected, 1182.18.

Analysis

$^1\text{H-NMR}$ spectra were recorded on an Avance AV 400-MHz digital Fourier transform NMR spectrometer with CDCl_3 as the solvent.



Scheme 2. Synthetic process of erythrosine B derivatives (R.T. = room temperature).

Ultraviolet–visible (UV–vis) spectra were recorded in dichloromethane solution with a Beijing Purkinje General TU-1901 UV–vis spectrophotometer.

Fluorescence spectra were recorded in a dichloromethane solution with an F-46001 Hitachi luminescence spectrophotometer with an excitation wavelength value of 490 nm.

Mass spectra were recorded with an LCQ fleet ion-trap mass spectrometer in positive electrospray mode. The electrospray voltage was 5 kV. The capillary temperature was 200°C, and the sheath gas was 30 units.

Photocalorimetry (photo-DSC)

The photopolymerization of HDDA and UVR were carried out with a differential scanning calorimeter (Q2000, TA Instruments) equipped with a photocalorimetric accessory (PCA OmniCure S2000, EXFO, Canada). Blue light was emitted from a 200-W mercury arc lamp through a 400–500-nm bandpass filter and was delivered by quartz light guides into the differential scanning calorimetry cell. An approximately 5.0-mg sample was placed in an aluminum Tzero pan, and a blank aluminum Tzero pan was used as a reference. Heat flow versus time curves were recorded in an isothermal mode under nitrogen or under an air flow of 50 mL/min. During the photopolymerization by photo-DSC, the sample was equilibrated at 25°C for the first minute, and subsequently, as the irradiation was carried out, the monitoring processes started. The reaction heat liberated in the polymerization was directly proportional to the number of vinyl groups or epoxy function groups reacting in the system. Through the integration of the area under the exothermic peak, the conversion (*C*) of the vinyl function groups or the extent of reaction could be determined according to the following equation:

$$C = \Delta H_t / \Delta H_{0\text{theor}}$$

where ΔH_t is the reaction heat evolved at time *t* and $\Delta H_{0\text{theor}}$ is the theoretical heat for the complete conversion of acrylic double bonds ($\Delta H_{0\text{theor}} = 86 \text{ kJ/mol}$).⁹

RESULTS AND DISCUSSION

Photophysical Characteristics

As shown in Figure 1, when the two susceptible groups of erythrosine B were modified, the obtained derivatives, EB0-B, EB4-B, EB0-EDB, and EB4-EDB, were greatly blueshifted in the visible region, and their molar extinction coefficients were lowered dramatically compared to the that of parent compound, EB. However, the spectrum of EB0 with only the modified carboxyl group was slightly redshifted compared to that of EB. So, we concluded that the modification of the phenolic group disturbed the chromophore of EB more strongly than the modification of the carboxyl group. Although the molar extinction coefficient of the synthesized derivatives exhibited small differences, their spectral shapes remained unchanged and were not affected by the specific ester and acylation groups; they also could overlap with the irradiation of the 400–500-nm light source.

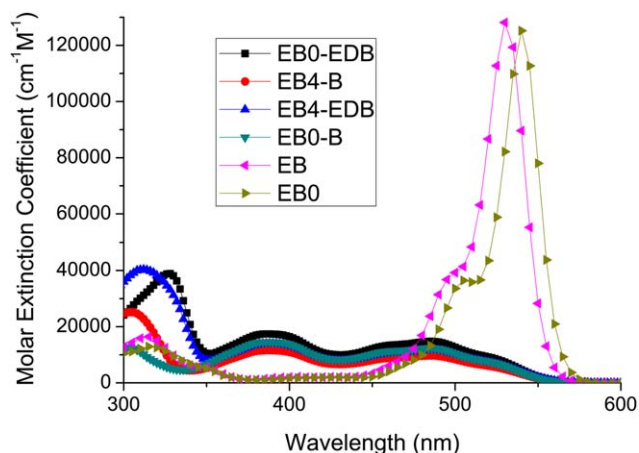


Figure 1. UV–vis absorption spectra of the synthesized derivatives in a dichloromethane solution. [Color figure can be viewed in the online issue, which is available at wileyonlinelibrary.com.]

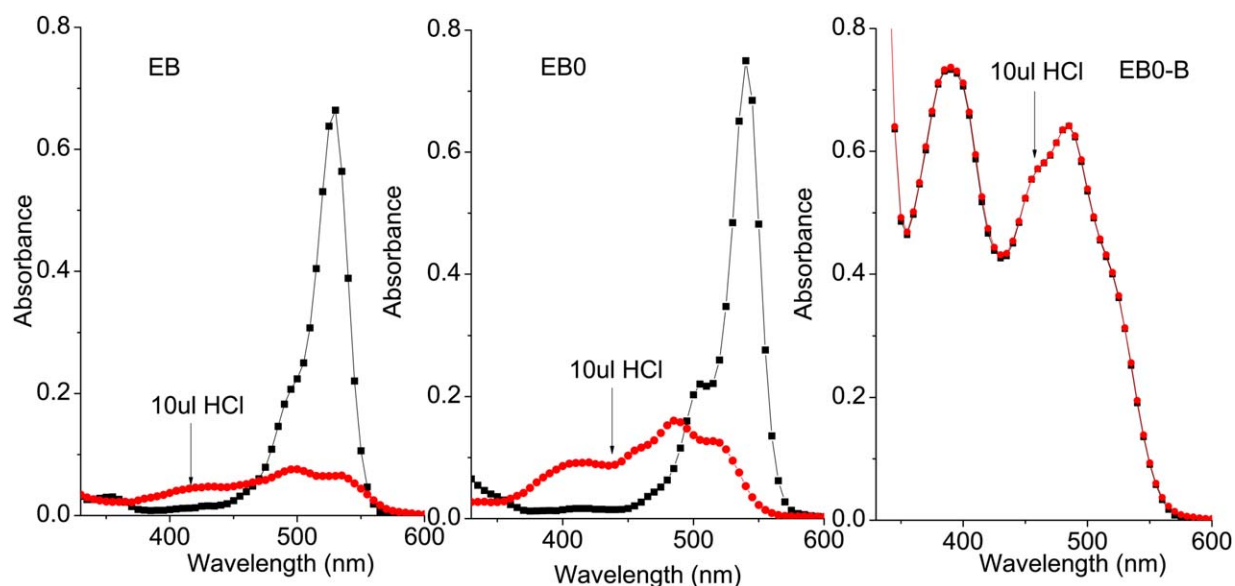


Figure 2. Spectral changes of EB in water, EB0 in methanol, and EB0-B in dichloromethane after the addition of 10 μL of HCl to the respective solutions. [Color figure can be viewed in the online issue, which is available at wileyonlinelibrary.com.]

Under alkaline conditions, EB and EB0, existing in the form of salts with one negative charge delocalized throughout a xanthenic nucleus, had nonfixed quinonoid structures and showed structural symmetry;¹⁰ they presented strong absorption peaks in the visible region. However, in an acid medium, EB existing in lactone form and EB0 with un-ionized hydroxyl groups¹¹ exhibited completely different absorption spectra, as illustrated in Figure 2. The derivatives with the two susceptible groups modified all of the exhibited excellent spectral stabilities in the acid medium. Thus, as photosensitizers, they could be used under different environmental conditions.

The fluorescence quenching of EB0-B at 500 nm by various concentrations of iodonium salt in dichloromethane was treated with the Stern–Volmer equation. The data fit this equation reasonably well, as shown in Figure 3. With the fluorescence lifetime assumed to be 0.1 ns on the basis of that of EB,⁴ the rate constant of fluorescence quenching was estimated to be $4 \times 10^{13} \text{ M}^{-1} \text{ s}^{-1}$. This large quenching constant suggested a rapid reaction between EB0-B and IOD in solution. It has been extensively reported that the fluorescence of the xanthenic dyes was quenched by IOD more efficiently than by tertiary amine in the three-component system, xanthenic dye/tertiary amine/IOD.⁶ Similarly, in our experiments, any significant fluorescence quenching was not observed in the solutions containing EB0-B and EDB; this indicated that the reaction rate between them was much slower. This information helped us to infer the synergistic mechanism of the EB0-B/EDB/IOD system for photopolymerization.

Free-Radical Photopolymerization Initiated by the Synthesized Derivatives

The derivatives bearing a coinitiator, EB4-EDB or EB4-B, as a single component were capable of initiating the free-radical photopolymerization of HDDA, and EB4-EDB exhibited a

higher photoinitiating efficiency than EB4-B [Figure 4(A)]; this was most likely because of the higher local concentration of the coinitiator. Interestingly, when we used EB0-EDB with a linked coinitiator at the phenolic hydroxyl position as the photoinitiator, no significant photopolymerization was observed; this indicated that this system did not produce active initiating centers. From observation of the molecular structure, it appeared that the coinitiator part of EB0-EDB was closer to its sensitizer part, as opposed to EB4-B, and thus, EB0-EDB should have shown more excellent photoinitiating ability. Moreover, even when there were no intramolecular reactions in EB0-EDB, the intermolecular reaction should have generated tertiary amine radicals for

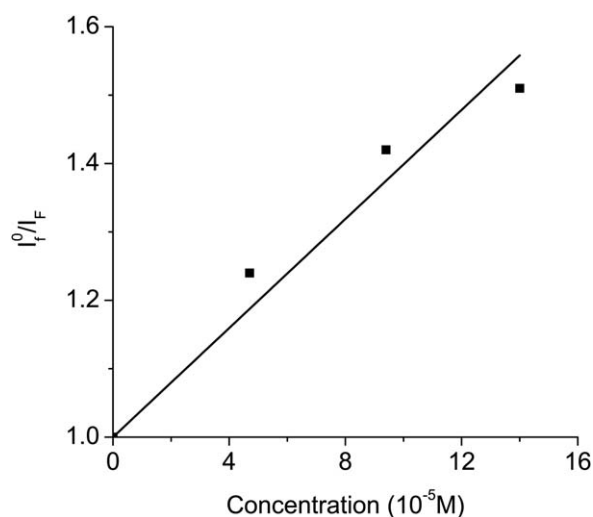


Figure 3. Stern–Volmer plot for the quenching of the fluorescence of EB0-B ($4.02 \times 10^{-5} \text{ M}$) by IOD in a dichloromethane solution (excitation wavelength = 490 nm) I_0^f was the fluorescence intensity of the solution without IOD and I_f was the one of the solution with IOD.

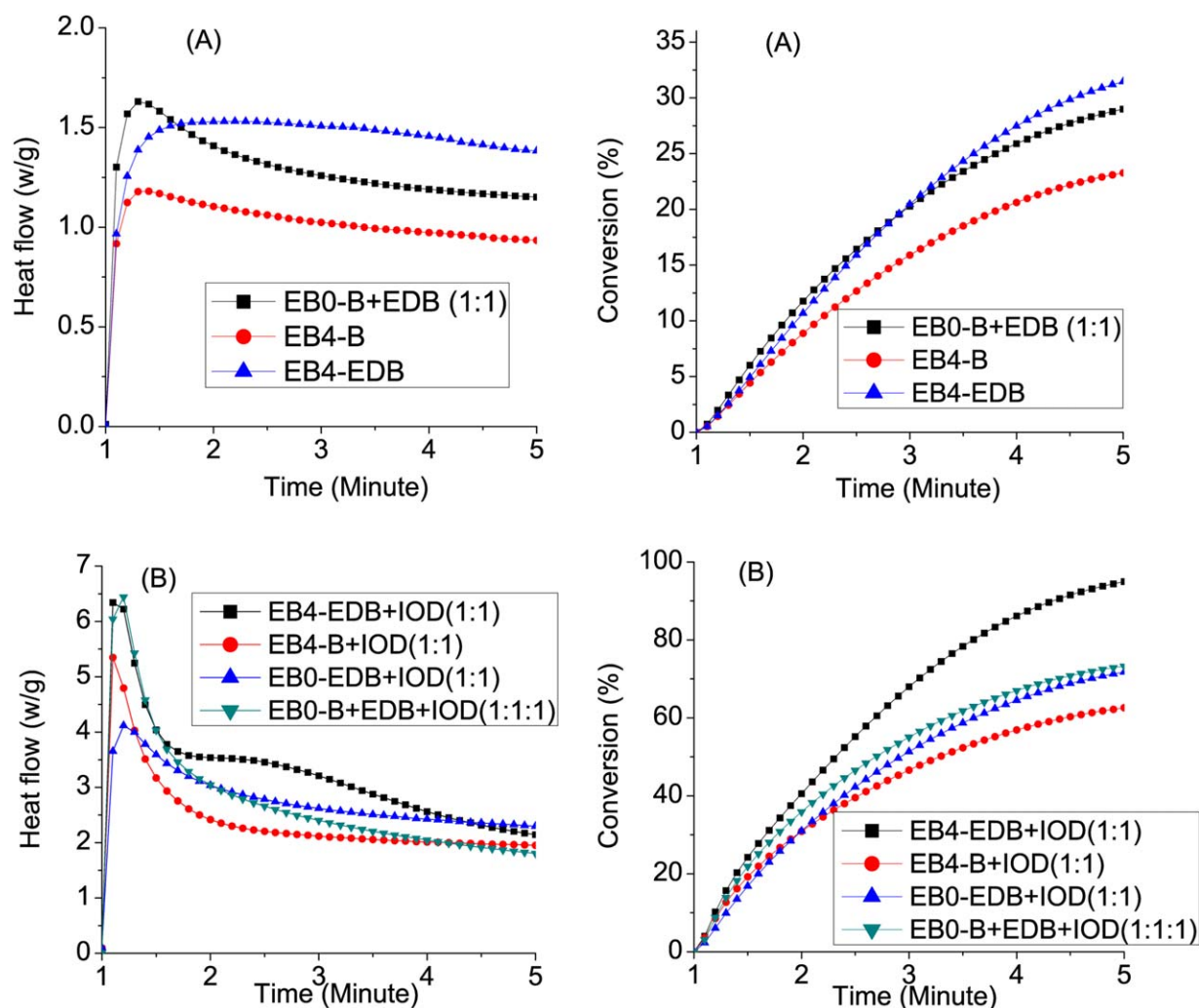


Figure 4. Photo-DSC profiles and conversion curves for the photopolymerization of HDDA initiated by (A) EB0-B/EDB, EB4-B, and EB4-EDB and (B) EB0-B/EDB/IOD, EB4-B/IOD, EB0-EDB/IOD, and EB4-EDB/IOD under a nitrogen atmosphere and visible light with an intensity of 71 mW/cm². For all systems, the concentration of the derivative was 0.5% w/w, and every component of the system was mixed in a 1:1 molar ratio. [Color figure can be viewed in the online issue, which is available at wileyonlinelibrary.com.]

photopolymerization. However, no polymerization occurred, and the only reasonable explanation was that on irradiation, the feasible back electron transfer¹² in EB0-EDB prevented the generation of tertiary-amine-initiating radicals. These results suggest that the phenolic position of EB was unsuitable for linking a coinitiator.

We observed that the separated two-component system EB0-B/EDB presented a better exothermic curve than the dye-linked one. In our previous study,¹³ when EDB was linked to the carboxyl position of EB, spaced by two methylene groups, the obtained dye-linked photoinitiator showed superiority over the separated counterpart in photopolymerization. Therefore, the longer linkage distance between these two parts in EB4-B were responsible for its relatively poor photoinitiating ability compared to that of EB0-B/EDB.

When combined with equimolar IOD [Figure 4(B)], the investigated derivatives exhibited a dramatically improved photoinitiating efficiency; this indicated a synergistic effect.

Their initiating ability retained almost the same trend in the absence of IOD. Interestingly, EB0-EDB combined with IOD showed a certain photoinitiating ability, as opposed to EB0-EDB alone; this indicated that IOD blocked the back electron transfer path to produce the tertiary amine radicals for polymerization.

Although the incorporation of IOD dramatically enhanced the photoinitiating efficiency of these derivatives, further increases in its amount did not bring about any significant promotion in the initiating ability, as illustrated in Figure 5(A). When additional EDB was incorporated into this system, remarkable promotion results were observed. However, continuous addition of only EDB also did not result in the expected improvement of the initiating efficiency (data are not shown). So there existed an interdependence between EDB and IOD in promoting the initiating efficiency; this provided some information about their synergistic mechanism.

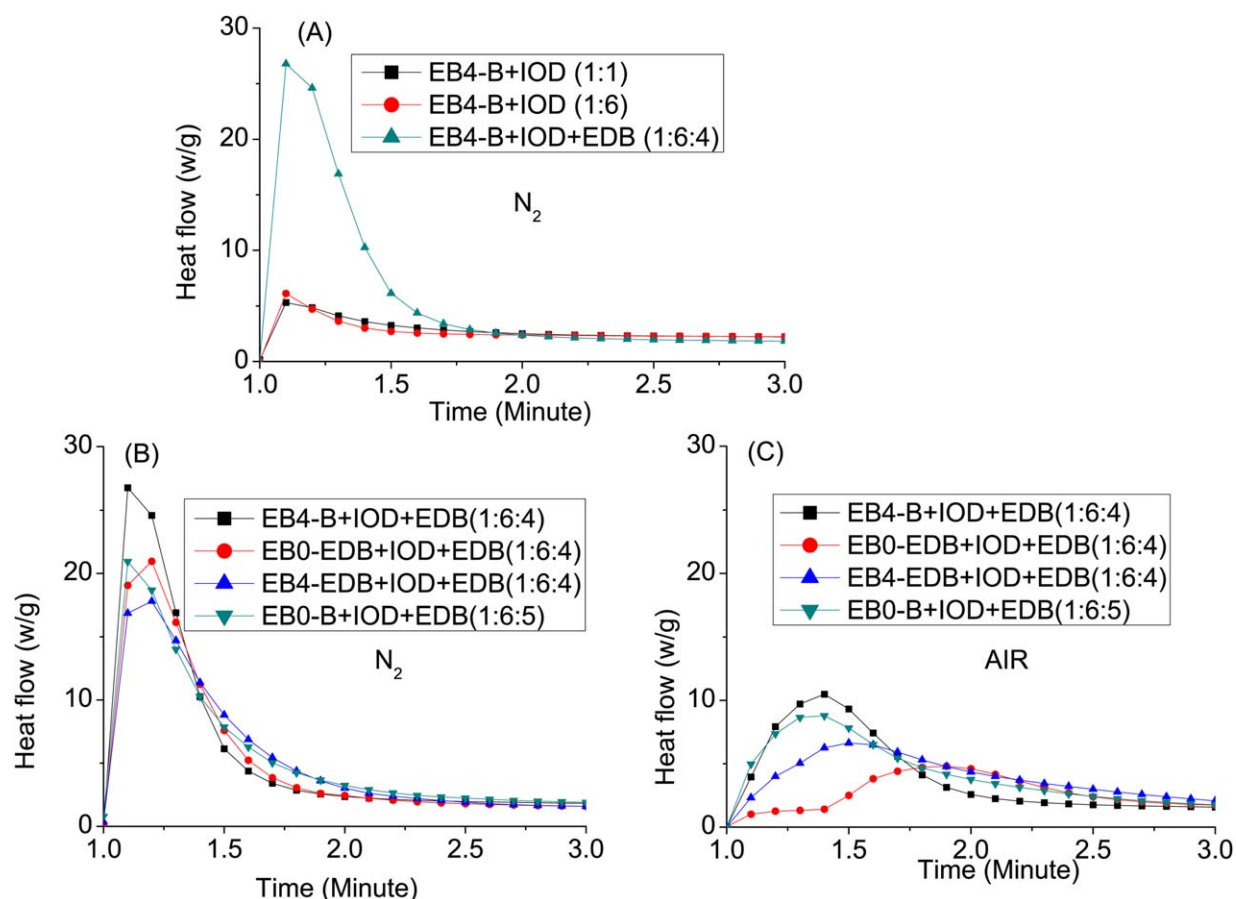


Figure 5. (A) Interdependent relationship between IOD and EDB in enhancing the photoinitiating efficiency under a nitrogen atmosphere and (B,C) photo-DSC profiles for the photopolymerization of HDDA initiated by EB0-B/IOD/EDB, EB4-B/IOD/EDB, EB0-EDB/IOD/EDB, and EB4-EDB/IOD/EDB under a nitrogen atmosphere and air, respectively. For all photoinitiating systems, the concentration of the derivative was 0.5% w/w, every component of the system was mixed in a molar ratio, and the photopolymerization was performed under visible light with an intensity of 71 mW/cm². [Color figure can be viewed in the online issue, which is available at wileyonlinelibrary.com.]

On the basis of the previous analysis, when the IOD and free EDB were added to this three-component system, dramatically enhanced kinetic profiles were obtained, as shown in Figure 5(B). We observed that the EB4-B displayed the best photoinitiating efficiency, and the EB4-EDB fell behind other systems. In this high-rate polymerization, the initially fast polymerization resulted in the moment vitrification of the resin and generated some free volumes with a certain size because of the volume shrinkage; this only allowed the diffusion of molecules with a relatively small size. Therefore, it became difficult for the diffusion of the EB4-EDB with its relatively larger molecular size to lead to its decreasing initiating ability. Jiang *et al.*¹⁴ reported that a microphotoinitiator with bulk size was did not favor the photoinitiating efficiency because of its limited movement. For the EB4-B system in the gel phase of initial polymerization, the vicinity between the reactant components may have been responsible for its excellent initiating efficiency. So, in this highly efficient polymerization formulation, this dye-linked photoinitiator showed an obvious advantage over the separated counterpart and had the potential for application. When polymerization occurred under air, the polymerization curves

dropped dramatically [Figure 5(C)]; this indicated a radical polymerization nature that was susceptible to oxygen.

Free-Radical-Promoted Cationic Photopolymerization Initiated by the Synthesized Derivatives

When onium salt, a typical iodonium salt, was incorporated into the common radical photoinitiator, the obtained system acquires the ability to initiate cationic polymerization. With this well-known strategy,¹⁵ derivatives/EDB/IOD systems were used to initiate the cationic ring-opening polymerization, and their exothermic curves are illustrated in Figure 6(A). As shown, they all exhibited excellent photoinitiating efficiency; this decreased in the order EB0-B > EB4-B > EB4-EDB > EB0-EDB. Simultaneously, curing samples with tack-free surfaces were obtained for all of the systems.

In the ring-opening polymerization of UVR, the system with EB0-B emerged as the most efficient photoinitiating system; this was different from the previous radical polymerization. Voytekunas *et al.*¹⁶ suggested that in cationic photopolymerization, the enhanced photoinitiating efficiency by the temperature was attributed to the increasing mobility of active species. Golaz

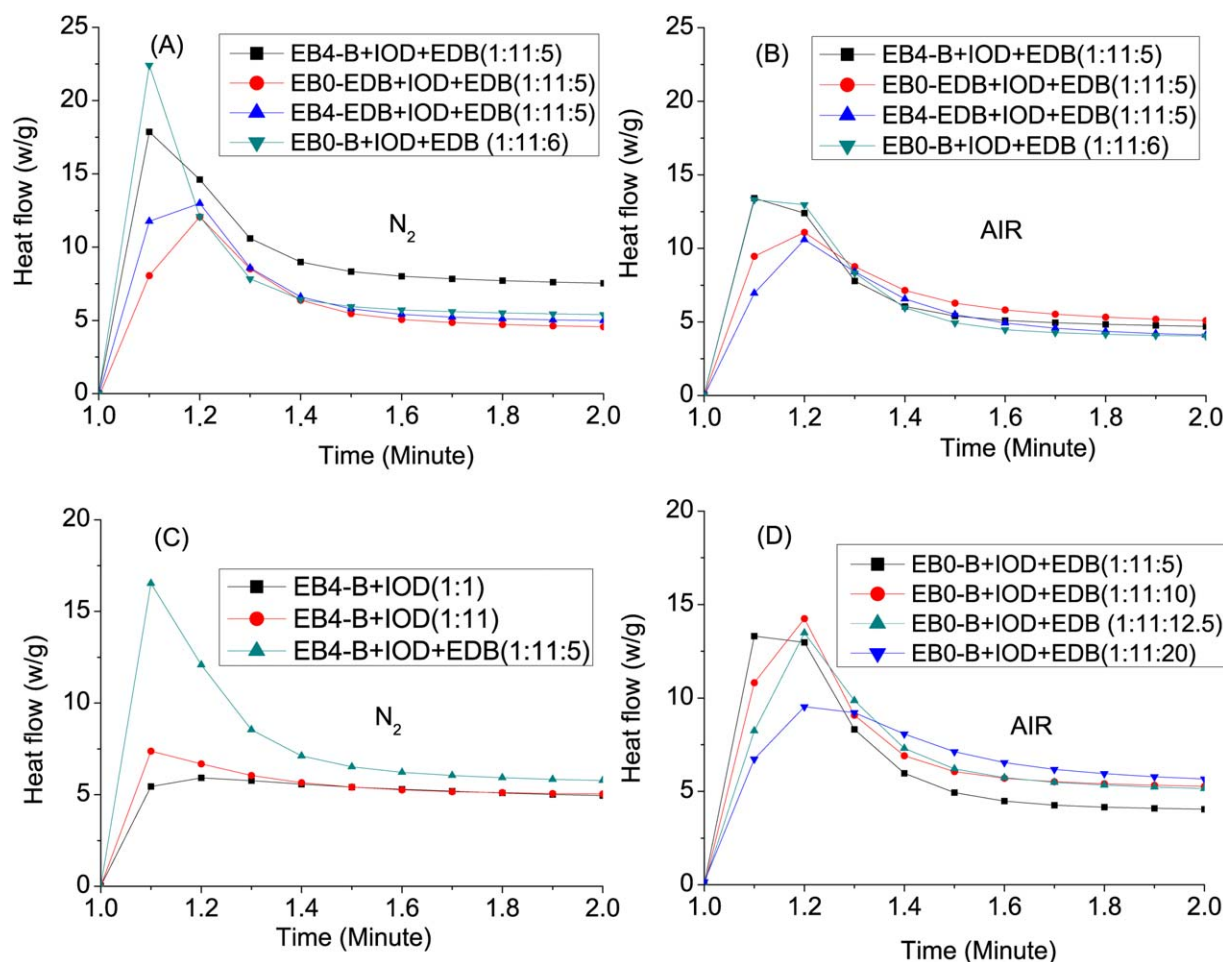


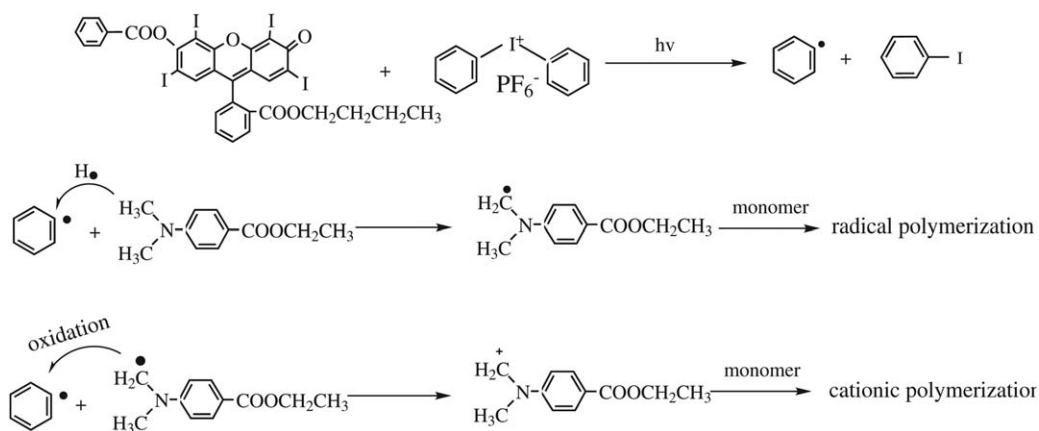
Figure 6. Photo-DSC profiles for the photopolymerization of UVR initiated by EB0-B/IOD/EDB, EB4-B/IOD/EDB, EB0-EDB/IOD/EDB, and EB4-EDB/IOD/EDB under (A) a nitrogen atmosphere and (B) air, (C) independent relationship between EDB and IOD in enhancing the photoinitiating efficiency under a nitrogen atmosphere, and (D) effect of increasing EDB on the photoinitiating efficiency under air. For all photoinitiating systems, the concentration of the derivative was 0.5% w/w, every component was mixed in a molar ratio, and the photopolymerization was performed under visible light with an intensity of 320 mW/cm². [Color figure can be viewed in the online issue, which is available at wileyonlinelibrary.com.]

*et al.*¹⁷ proposed that the special dark-curing behavior in cationic photopolymerization enabled the conversion to be further improved; this was caused by the diffusion of activated photoinitiators. These facts indicated that after the initial vitrification, the movement of active species was very important for further curing. So, the small and mobile reactant component in EB0-B/IOD/EDB was responsible for its higher initiating efficiency, and the relatively slower diffusion of EB4-EDB was responsible for its lower photoinitiating efficiency. The system with EB0-EDB, whether in cationic or radical photopolymerization, all displayed poor initiating performance; this indicated that the modification of the phenolic hydroxyl position of EB by the linking of a coinitiator resulted in a negative effect on its initiating ability.

Although the ring-opening polymerization of UVR was initiated by cationic active species insensitive to oxygen, the maximum heat flow of the investigated systems [Figure 6(B)] dropped under air; this indicated that on irradiation, this system produced radicals, which might have been the intermediate for

forming cationic active species, and was insensitive to oxygen; this resulted in the reduction of the photoinitiating efficiency.

Although IOD is usually used as a photoinitiator for cationic polymerization,¹⁸ the excessive addition of IOD could not give a larger promotion to the initiating ability of the EB4-B/IOD, as illustrated in Figure 6(C). Just as the previous studies on the radical promoted cationic polymerization,¹⁹ the introduction of the tertiary amine (EDB) strongly promoted the photoinitiating efficiency of cationic polymerization. However, with the continuous addition of EDB to EB0-B/IOD to the cationic photopolymerization under air [Figure 6(D)], the photoinitiating efficiency shows a trend of increase first and then decrease; this indicated that there existed an optimum proportion, and the excessive addition of EDB was unfavorable for cationic photopolymerization. For the free-radical photopolymerization initiated by the same photoinitiator EB0-B/EDB/IOD, we found that the excessive addition of IOD had a negative effect on the photoinitiating efficiency (data not shown). This phenomenon was observed in our previous study.²⁰ These differences



Scheme 3. Mechanism.

delivered important information on the photoinitiating mechanism of this system.

Synergistic Mechanism

As mentioned previously, the fluorescence of EB0-B was strongly quenched by IOD but not by EDB. So, we concluded that in EB0-B/EDB/IOD, on exposure to irradiation, EB0-B/IOD had a faster reaction rate than EB0-B/EDB.

Therefore, for the EB0-B/EDB/IOD, the photochemical reaction between EB0-B and IOD resulted in the photolysis of IOD to produce active phenyl radicals. This conclusion was supported by the work of Neckers¹¹ on the photo-induced electron transfer between erythrosine B ethyl ester and IOD. Although the phenyl radical was very active, it could not initiate free-radical polymerization effectively.⁶ We proposed that the most crucial role of the phenyl free-radical was to oxidize the tertiary amine to α -amine initiating radicals for free-radical polymerization.¹³ Bi and Neckers²¹ reported that a diphenyliodonium salt in conjunction with an amine could be used as an effective photoinitiating system for free-radical polymerization under UV irradiation. In this system, on UV irradiation, the photolysis of diphenyliodonium salt produced the phenyl radical, which abstracted a hydrogen from an amine to yield an α -amine radical for radical polymerization. Moreover, on the basis of this mechanism, the independence between EDB and IOD in enhancing the photoinitiating efficiency of the EB0-B/EDB/IOD for free-radical polymerization could be reasonably explained.

For the radical-promoted cationic photopolymerization of the three-component system containing IOD, two different mechanisms were reported.^{1,8,22,23} One suggested that the free radicals first produced by this system were directly oxidized by the iodonium salt to corresponding cationic centers for the ring-opening polymerization of epoxy monomers. The other was that the phenyl radical from the photolysis of the iodonium salt oxidized the α -amine radical to cationic active centers. As mentioned, the phenyl radical from the photolysis of the iodonium salt possessed the ability to oxidize tertiary amine. Without any external energy, there was no reaction between the iodonium salt and amine. As an electron-defect compound, the α -amine radical was more difficult to oxidize than the original amine. Therefore, we reasonably concluded that the phenyl radical

rather than iodonium salt was still responsible for further oxidizing the α -amine radical to the corresponding cationic active species for the cationic photopolymerization. Thus, during the ring-opening photopolymerization initiated by EB0-B/EDB/IOD under air, the excessive EDB continuously consumed the phenyl radical to produce a large number of α -amine radicals sensitive to oxygen. Because of the lack of enough oxidizer (phenyl radical), the subsequent further oxidation of α -amine radicals to α -amine cationic active species was blocked; this resulted in a low efficiency for the cationic polymerization [Figure 6(D)]. Therefore, the excessive EDB in EB0-B/EDB/IOD did not favor the cationic photopolymerization. The mechanism of the free-radical-promoted cationic photopolymerization and free-radical photopolymerization initiated by the same system EB0-B/EDB/IOD is shown in Scheme 3. On the basis of this mechanism, the excessive IOD in EB0-B/EDB/IOD generated a large amount of phenyl radicals; these continuously oxidized the tertiary amine radical to α -amine cationic active species. Thus, the number of free-radical species decreased; this resulted in low efficiency for the free-radical polymerization. Therefore, excessive IOD in EB0-B/EDB/IOD did not favor the free-radical photopolymerization.

CONCLUSIONS

Three dye-linked photoinitiators were synthesized; these were characterized by the coinitiator moiety linked to the phenolic group of erythrosine B, the carboxylate group, or both. They all showed high-spectrum stability in an acid medium. The derivative with two linked coinitiators exhibited a higher photoinitiating efficiency for radical polymerization whether in the absence or presence of an equimolar amount of iodonium salt. However, in the polymerization formulation with additional free coinitiator and iodonium salt, this derivative exhibited a relatively poorer photoinitiating efficiency for radical or cationic polymerization because of the limited mobility caused by its larger molecular size. Compared to the carboxylate group position of erythrosine B, the phenolic group linked with a coinitiator was not favorable for the promotion of the photoinitiating efficiency because of the strong back electron transfer. In the derivative/amine/iodonium salt system, the excessive iodonium salt had a negative effect on the free-radical photopolymerization, and the excessive tertiary

amine had a negative effect on the cationic photopolymerization; this provided useful information for the design of the corresponding photoinitiating system for these two polymerizations. We suggest that in this three-component system, it was the phenyl radical produced during the photochemical reaction that was responsible for oxidizing the tertiary amine to α -amine radicals for free-radical photopolymerization, and it was also responsible for the further oxidation of the α -amine radicals to cationic active centers for cationic photopolymerization. This mechanism could reasonably explain all of the experimental phenomena.

ACKNOWLEDGMENTS

The authors thank the National Natural Science Foundation of China (contract grant number 51273180), the Young Researchers Foundation of Zhejiang Provincial Top Key Academic Discipline of Chemical Engineering and Technology of Zhejiang Sci-Tech University (contract grant number ZYG2015009), and Zhejiang Provincial Top Key Discipline of Biology.

REFERENCES

1. Shao, J. Z.; Huang, Y.; Fan, Q. G. *Polym. Chem.* **2014**, *5*, 4195.
2. Tehfe, M.-A.; Dumur, F.; Xiao, P.; Graff, B.; Savary, F. M.; Fouassier, J. P.; Gigmes, D.; Lalevée, J. *Polym. Chem.* **2013**, *4*, 4234.
3. Fouassier, J. P.; Savary, F. M.; Lalevée, J.; Allonas, X.; Ley, C. *Materials* **2010**, *3*, 5130.
4. Encinas, M. V.; Rufs, A. M.; Bertolotti, S. G.; Previtali, C. M. *Polymer* **2009**, *50*, 2762.
5. He, J. H.; Li, M. Z.; Wang, J. X.; Wang, E. J. *J. Photochem. Photobiol. A* **1995**, *89*, 229.
6. Padon, K. S.; Scranton, A. B. *J. Polym. Sci. Part A: Polym. Chem.* **2001**, *39*, 715.
7. Kim, D.; Stansbury, J. W. *J. Polym. Sci. Part A: Polym. Chem.* **2009**, *47*, 887.
8. Bi, Y.; Neckers, D. C. *Macromolecules* **1994**, *27*, 3683.
9. Jiang, X. S.; Xu, H. J.; Yin, J. *Polymer* **2005**, *46*, 11079.
10. Amat-Guerri, F.; López-González, M. M. C.; Martínez-Utrilla, R.; Sastre, R. *Dyes Pigments* **1990**, *12*, 249.
11. Bi, Y.; Neckers, D. C. *J. Photochem. Photobiol. A* **1993**, *74*, 221.
12. Kim, D.; Scranton, A. *J. Polym. Sci. Part A: Polym. Chem.* **2004**, *42*, 5863.
13. Nan, X. Y.; Huang, Y.; Fan, Q. G.; Shao, J. Z. *Prog. Org. Coat.* **2015**, *81*, 11.
14. Jiang, X. S.; Wang, W. F.; Xu, H. J.; Yin, J. *J. Photochem. Photobiol. A* **2006**, *181*, 233.
15. Yagci, Y.; Schnabel, W. *Chem. Macromol. Symp.* **1992**, *60*, 133.
16. Voytekunas, V. Y.; Ng, F. L.; Abadie, M. J. M. *Eur. Polym. J.* **2008**, *44*, 3640.
17. Golaz, B.; Michaud, V.; Leterrier, Y.; Manson, J.-A. E. *Polymer* **2012**, *53*, 2038.
18. Crivello, J. V. *J. Polym. Sci. Part A: Polym. Chem.* **1999**, *37*, 4241.
19. Schroeder, W. F.; Asmussen, S. V.; Sangermano, M.; Vallo, C. I. *Polym. Int.* **2013**, *62*, 1368.
20. Nan, X. Y.; Huang, Y.; Fan, Q. G.; Shao, J. Z. *J. Appl. Polym. Sci.* **2015**, *132*, 42361.
21. Bi, Y.; Neckers, D. C. *Tetrahedron Lett.* **1992**, *33*, 1139.
22. Lalevée, J.; Tehfe, M.; Zein-Fakih, A.; Ball, B.; Telitel, S.; Morlet-Savary, F.; Graff, B.; Fouassier, J. P. *Macro Lett.* **2012**, *1*, 802.
23. Lalevée, J.; Telitel, S.; Xiao, P.; Lepeltier, M.; Dumur, F.; Morlet-Savary, F.; Gigmes, D.; Fouassier, J. P. *Beilstein J. Org. Chem.* **2014**, *10*, 863.